WELLBORE INSTABILITY EVALUATION BY USING MOHR-COULOMB FAILURE CRITERION [+]

AbdulKarim Abbas Al-Rubaey [*] **Akrim Hamoudy Al-Hiti** [**]

Abstract :

Wellbore instability represent one of the serious drilling problems encountered in shale formations due to interaction between drilling fluids and shale formations. The investigated Shale samples was taken from Well (K-246) located in Baba Dome in Kirkuk oil field.

Pore pressure transmission experiments were performed to study the effect of variations in wellbore pressure (P_w) with different salt types and concentrations on the wellbore pressure(P_{nw}) which affect or disturb the state of stresses around the wellbore.

The Invariant Shear Stress ($\sqrt{J_2}$) profile are calculated to determine wellbore instability state as a function of salt types and concentrations depending on the Mohr-Coulomb failure criterion which is experimentally determined for the shale sample by Tri-axial Test. The results shows that well (K-246) is unstable(Collapse Failure) at (P_w = 2400 psi and 2440 psi) at salt concentration (14% and 16%) for NaCl, KCl and $CaCl_2$ salt solutions but stable for other salt concentrations employed in the research.

Key words: Wellbore instability, Invariant shear stress, Mohr-Coulomb failure criterion, Pore pressure transmission test.

تقييم عدم إستقرارية البئر النفطي باستخدام خاصية الانهيار لمور_ كولومب

عبد الكريم عباس الربيعي اكرم حمودي الهيتى

المستخلص :

تعتبر مشكلة عدم استقرارية البئر النفطي إحد اخطر مشاكل الحفر في طبقات الطَفَل بسبب التداخل بين سوائل الحفر وهذه الطبقات . النموذج الذي تم استخدامه في البحث هو للبئر رقم (ك-246) الواقع في قبة بابا في حقل كركوك النفطي.اجريت تجارب لتحديد انتقال الضغط المسامي لدراسة تاثير اختلاف ضغط البئر باختلاف تراكيز وانواع الاملاح المستخدمة على الضغط المسامي القريب من البئر والذى يؤثر ويغير من حالة الاجهادات حول البئر.

أُجريت تجارب انتقال الضغط المسامي لدراسة تاثير تغيّر الضغط عند جدار البئر مع محاليل ملحية وبتراكيز مختلفة لكلوريد الصوديوم وكلوريد البوتاسيوم وكلوريد الكالسيوم على الضغط القريب من البئر والذي يؤثر او يغير من حالة الاجهادات حول البئر النفطي.

تم حساب منحنى إجهاد القص غير المتغير لتحديد حالة عدم استقرارية البئر كدالة لتغير نوع وتراكيز الأملاح المستخدمة بالاستناد على خاصية الفشل بطريقة(مور – كولومب) التي تم قياسها مختبريا لنموذج الطفل باستخدام

[+] Received on 8/1/2014 , Accepted on 30/12/2014

[*] Assistant Prof. / Technical College / Musayab / Al-Furat Al-Awsat Technical University

[**] Professor / College of Engineering / Baghdad University

البحث مستل من إطروحة الدكتوراه للباحث الأول

اختبار الاجهاد ثلاثي- المحاور . اظهرت النتائج بأن البئر (ك- 246) يكون غير مُستقر عند ضغط البئر (2400 باوند / إنج^2 و 2440 باوند / إنج^2) عند التراكيز (14% و 16%) لأملاح كلوريدات الصوديوم والبوتاسيوم والكالسيوم ويكون البئر مستقرا عند التراكيز الاخرى .

1. Introduction :

The most challenging problems related to drilling shale formations are wellbore instability. Wellbore instability problems cost the petroleum industry an estimated (500) million USD per year. [1]. Wellbore instability is still a serious problem not only in the petroleum industry, but also in the mining and construction industries. [2].
Failures occurs due to wellbore instability problems are tensile, compressive and shear failure. The mode of failure depends on the mechanical and physicochemical properties of the shale rock. [3];[4].
Numerous factors cause wellbore instability such as: [5];[6];[7].

1. In-situ stress state conditions.
2. Well type (vertical or directional).
3. Well trajectories (inclination and azimuth).
4. Rock properties (Strength, Poisson ratio, Modulus of elasticity, Permeability and Porosity).
5. Shale / drilling fluids interaction.
6. Thermal effects [8].

These factors can be classified as mechanical, chemical and thermal effects where some of these factors are controllable the others are uncontrollable.

The objectives of the research is to estimate:

1. The membrane efficiency of the shale sample due to interaction between different drilling fluids and the shale formation.
2. The change in near wellbore pressure as a chemical stresses effects on the mechanical stress state around the wellbore.
3. To develop an invariant shear stress profile to depicts the instability state around the wellbore using Mohr_ Coulomb Failure Criterion.

2. Wellbore Stability Analysis :

Shale is a fine-grained rock containing a sizable fraction of clay minerals which greatly influence shale chemical behaviors in the presence of aqueous solutions. Montmorillonite is the only clay minerals that has a water interlayer and thus exhibits swelling tendency where the unit layer of Montmorillonite can vary from (9.7 Å) to (17.2 Å) [9];[10];[11]. So the Cation Exchange Capacity (CEC) should influence the shale membrane efficiency and ion selectivity.
The ideality of shale membrane efficiency (I_m) is a function of the cation exchange capacity, porosity and salts concentrations of the pore fluid. (I_m) can be defined as [12];[13].

$$I_m = \frac{\Delta P_{observed}}{\Delta P_{theoretical}} \times 100\% \quad \ldots\ldots (1)$$

$$\Delta P_{th} = \frac{RT}{V_w} ln \frac{a_{w\ sh.}}{a_{wdf}} \quad \ldots\ldots (2)$$

Where:

R- gas constant, Lit. atm./mole. K°.
T- temperature, K°.
V_w- molar volume of water, Lit./mole.
a_{wsh}- shale water activity.
a_{wdf}- drilling fluid water activity.
I_m- shale membrane efficiency.
ΔP- pressure difference, psi.

The mechanical stresses effects on the wellbore instability may be defined by determining in-situ stresses, rock strength and bedding planes. The total stress state around a wellbore as governed by in-situ stresses and hydraulic effect derived as shown in Appendix (A) [13];[14]. If the consequence of interactions of chemical effects and membrane efficiency of the shale formation due to osmosis is coupled with the distribution of mechanical stresses in the vicinity of the borehole wall, the equations of stress model become: [15].

$$\sigma_{rr} = P_w - P_{nw} \quad \ldots\ldots (3)$$

$$\sigma_{\theta\theta} = \sigma_x + \sigma_y - P_w - 2(\sigma_x - \sigma_y)\cos 2\theta - 4\tau_{xy}\sin 2\theta + \alpha\Delta P - I_m \Delta P - P_{nw} \quad \ldots\ldots (4)$$

$$\sigma_{zz} = \sigma_z - \nu\left[2(\sigma_x - \sigma_y)\cos 2\theta + 4\tau_{xy}\sin 2\theta\right] + \alpha\Delta P - I_m \Delta P - P_{nw} \quad \ldots\ldots (5)$$

$$\tau_{r\theta} = \tau_{rz} = \tau_{\theta z} = 0 \quad \ldots\ldots (6)$$

And:

$$P_{nw} - P_o = I_m \times \Delta P = I_m \frac{RT}{V_w} ln \frac{a_{wsh}}{a_{wdf}} \quad \ldots\ldots (7)$$

The failure criterion must be considered to define the state of failure around the wellbore wall which represent the equilibrium state between the shear stresses around the wellbore and the compressive strength of the rock. The simplest and most popular criterion that was introduced by Coulomb [16] defined as:

$$\tau = C_o + \mu\sigma \quad \ldots\ldots (8)$$

$$C_o = \frac{UCS}{2(\sqrt{1+\mu^2} + \mu)} \quad \ldots\ldots (9)$$

$$\mu = \tan\phi \quad \ldots\ldots (10)$$

Where:

C_o = the cohesive strength, psi.
ϕ = the friction angle, degree.
UCS = uni-axial compressive strength, psi.
μ = the coefficient of friction angle.

The invariant shear stress around the wellbore which represent the actual shear stresses around the wellbore ($\sqrt{J_2}$) can be calculated by the following equations [17].

$$J_1^{eff} = \frac{\sigma_{rr} + \sigma_{\theta\theta} + \sigma_{zz}}{3} \quad \ldots\ldots \quad (11)$$

$$\sqrt{J_2} = \sqrt{\frac{1}{9}\left[(\sigma_{rr} - \sigma_{\theta\theta})^2 + (\sigma_{\theta\theta} - \sigma_{zz})^2 + (\sigma_{zz} - \sigma_{rr})^2\right] + \tau_{r\theta}^2 + \tau_{\theta z}^2 + \tau_{rz}^2} \quad \ldots\ldots \quad (12)$$

Where:

J_1^{eff} - effective mean stress, psi.

$\sqrt{J_2}$ – invariant shear stress, psi.

3. Experimental Work :

The pressure transmission technique is applied to measure the osmotic pressure difference (ΔP) across the shale sample and to measure the variations in near wellbore pressure due to interaction between drilling fluids and shale formation. Fig. 1 shows the experimental setup and equipment components used to carry out the test.[18].

The test procedure is summarized by injecting the downstream simulated pore fluid having a water activity (0.92) to saturate the shale core sample (1" × 2") which is placed in the main cell shown in Fig.2 by injection pump. Salt solutions with different salt concentrations as drilling fluid (with different water activity) injected by the upstream injection pump, with different wellbore pressure (P_w). The change (reduction) in osmotic pressure or near wellbore pressure (P_{nw}) is monitored continuously with time.

Twenty two experiments are conducted to measure the osmotic pressure to calculate the membrane efficiency of the shale sample. (96) experiments performed is to measure the change in near wellbore pressure with time due to interaction between drilling fluid with different salt concentrations and salt types with shale sample.

4. Results and Discussion :

The membrane efficiency tests are conducted to measure the variation or build up of the downstream pressure with time during the injection of the upstream drilling fluids (salt solutions). The difference between the upstream and the downstream pressure (ΔP) was calculated which represents the induced osmotic pressure which are used to calculate the membrane efficiency of the shale sample as shown in Fig. 3 for NaCl salt solutions, Fig. 4 for KCl salt solutions and Fig. 6 for $CaCl_2$ salt solutions respectively.

The membrane efficiency calculations is illustrated by an example for (4%) NaCl salt solutions with (0.98) water activity as an upstream drilling fluid. Eq. (3) calculates the theoretical osmotic pressure which equal to (– 1375.87 psi). the difference between the upstream drilling fluid pressure and the downstream pressure during the test measured as (ΔP) which represent the observed osmotic pressure (– 120 psi) for (4%) NaCl. So the membrane efficiency calculated by eq. (3) gives (I_m = 8.72%).

The membrane efficiency values for other salt solutions are calculated and tabulated in Table 1. The negative sign for observed osmotic pressure occurred when the water activity for the drilling fluid is greater than the shale water activity. This may be due to the combined flux of

water from the wellbore into the shale formation by hydraulic and osmotic pressure potentials. In other tests where the drilling fluids water activity is less than (a_{wsh}), the osmotic pressure potential was offsetting some of the hydraulic potential which make the downstream pressure always less than the circulating upstream pressure as shown for (14%) NaCl salt solution with (a_w = 0.9) which gives (ΔP = 32 psi), (ΔP_{th} = 478.64 psi).So the membrane efficiency is equal to (I_m = 6.68%).

Generally as shown in Table 1, as the water activity of the salt concentrations decreases, (ΔP) observed osmotic pressure increases and the membrane efficiency decreases. This may be attributed to the reduction in the amount of water that can be transported to the shale formation due to reduction of water activity and the reduction in chemical potential gradient between the drilling fluid and shale formation water activity. So all the values of the observed osmotic pressure and membrane efficiency are generally low.

The KCl salt solutions tests indicates the lowest membrane efficiency values compared with NaCl and $CaCl_2$ solutions because the (K^+) cations average hydrated radius (5.32 Å) is smaller than the hydrated radius of (Na^+) cations (7.9 Å) and (Ca^{++}) cations (9.6 Å).

Pore pressure transmission tests are performed in order to study the effect of variations in wellbore pressure (P_w) as drilling mud density with different salt types and concentration on the near wellbore pressure (P_{nw}) which affect or disturb the state of stresses around the wellbore. The tests utilized four different values for wellbore pressure (2400 psi, 2440 psi, 2570 psi and 2700 psi) while the salt concentration ranging from (14% to 26%) for NaCl, KCl and $CaCl_2$ salt solutions.

Fig. 6 show the pore pressure transmission test for (14%) NaCl salt solutions at (P_w = 2400 psi) and ($P_{conf.}$ = 2800 psi). The test sample in the cell is subjected to a confining pressure (2800 psi) followed by a circulating solution (12%) NaCl to reach equilibrium after (10 hrs.), and (P_w) maintained at (2400 psi). Finally the shale is exposed to the test fluid (14%) NaCl and after (16 hrs.), the downstream pressure starts to reduce continuously until it stabilizes at (1430 psi) after (40 hrs.) which represent the effect of chemical potential difference on the near wellbore pressure (P_{nw}). The same tests for other salt types at different salt concentrations and for other wellbore pressure values are conducted.

To depicts the state of failure around the wellbore we must calculate the invariant shear stress profile ($\sqrt{J_2}$) and draw the invariant shear stress profile. In this research ($\sqrt{J_2}$) is calculated by introducing the mechanical and chemical stresses encountered around the wellbore as shown in Appendix (A). The invariant shear stress profile ($\sqrt{J_2}$) with % salt concentrations are shown in Figs. 7, 8, 9 for NaCl, KCl and $CaCl_2$ respectively.

These figures showed that:

1. The chemical factors represented by an osmotic phenomena due to difference in water activity between the drilling fluid and shale formation increase the ($\sqrt{J_2}$) values, so increase the instability of the wellbore.
2. The increase in salt concentrations cause to increase the instability of the wellbore due to reduction in (P_{nw}) because of increase in osmotic pressure due to osmosis phenomena.
3. There is a minimum salt concentration for each salt solution type that gives the most stability of the wellbore, i.e. the lowest values for ($\sqrt{J_2}$).
4. The failure envelope represented by Mohr-Coulomb failure criterion measured in the laboratory by tri-axial test for five core shale samples which gives an equation of a straight line as**:**

$$\boldsymbol{\tau} = \mathbf{0.503}\boldsymbol{\sigma} + \mathbf{803} \quad \ldots\ldots \quad (13)$$

This failure envelope line define the stability of the wellbore which represent the collapse failure around the wellbore.

5. The failure envelope line define the stable and unstable region for the wellbore so for NaCl salt solutions only (14% and 16%) at (P_w = 2400 psi) and (14%) at (P_w = 2440 psi) lies above the strait line, so these points reflect the instability of the wellbore, where the wellbore may be collapse. For KCl salt solutions (14% and 16%) gives instability of the wellbore at (P_w = 2400 psi and 2440 psi). For $CaCl_2$ solutions (14% and 16%) salt concentrations shows the instability of the wellbore at (P_w = 2400 psi and 2440 psi).

5. Conclusions :

1. All measured membrane efficiency values were low ranging from (1.41% to 9.8%).
2. As the water activity gradients increased (i.e. a_{wdf} decreased) the membrane efficiency decreased.
3. The chemical factors (osmosis phenomena) tends to raise the invariant shear stress values which in turn enhance wellbore instability in shale formations.
4. For each wellbore pressure (P_w), there is a minimum salt solution concentration that gives the lowest value for the invariant shear stress which represent the most stability of the wellbore.
5. Get the failure envelope line equation by Mohr-Coulomb theory for the region investigated.

6. References :

1. Mitchell, J., "*Trouble-Free Drilling*", Vol. 1, "*Stuck Pipe Prevention*", Ch. 8, "*Well Bore Instability*", Drillbert Engineering Inc. Copyright, pp. 111-185, 2001.
2. Jeager, J.C. and N.G. Cook, "Fundamentals of Rock Mechanics", Ed. Methuen & Co. LTD, London, 1969.
3. Bradley, W.B., "*Mathematical Concept-Stress Cloud Can Predict Borehole Failure*", Oil & Gas J., Vol. 77, No. 8, Feb. pp. 92-102.
4. Cook, J., "*The Effects of Pore Pressure on the Mechanical and Physical Properties of Shale"*, Oil and Gas Science & Tech. Rev. IFP, Vol. 54, No. 6, pp. 695-701, 1999.
5. McLellan, P.J., "Assessing the Risk of Wellbore Instability in Horizontal and Inclined Wells", JCPT, Vol. 35, No. 5, pp. 21-32, May 1996.
6. McLellan, P., C. Hawkes and Y. Yuan, "Minimizing Borehole Instability Risks in Build Sections Through Shales", Presented at the Conference on Horizontal Well Technology, Calgary, Alberta, Canada, Nov. 3, pp-1-15, 1999.
7. Tare, U.A. and F.K. Mody, "Managing Borehole Stability Problems: On the Learning, Unlearning and Relearning Curve", AADE-02-DFWM-HO-31, pp. 1-8, April 2002.
8. Maury, V.M. and J.M. Sauzay, "*Borehole Instability: Case Histories, Rock Mechanics Approach and Results*", SPE 16051, pp. 11-24, March 1987.
9. Folk, L. Robert "*Petrology of Sedimentary Rocks",* 2nd Ed., Austin, TX, Hemphill, 1947.
10. Blatt, Harvey and J. Robert, Tracy, "*Petrology: Igneous Sedimentary and Metamorphic*". 2nd Ed., New York: W. H. and Freeman Company, 1982.
11. Bassiouni, Zaki, "Theory, Measurement, and Interpretation of Well Logs", SPE Textbook series, Vol.4. Richardson, TX: SPE Inc., 1994.
12. Lal, M., "*Shales Stability: Drilling Fluid Interaction and Shale Strength*", SPE 54356, pp. 1-8, April 1999.
13. Schlemmer, R., J.E. Friedheim, F.B. Growcoch, J.E. Bloys, J.A. Headly and S.C. Polnaszek, "*Membrane Efficiency in Shale: An Empirical Evaluation of Drilling Chemistries and Implications for Fluid Design*", SPE 74557, pp. 1-10, Feb. 2002.
14. Fjaer, E., R.M. Holt, O.M. Nes and E.F. Sontabo, "*Mud Chemistry Effects on Time-Delayed Borehole Stability Problems in Shales*", SPE 78163 , pp. 1-9, Oct. 2002.
15. Mclean, M.R. and M.A. Addis, *"Wellbore Stability: The Effect of Strength Criteria on Mud Weight Recommendations",* SPE 20405, pp. 23-26, Sept. 1990.
16. Mody, F.K. and A.H. Hale, " *Chemistry of Drilling Fluid Shale Interaction",* SPE 25728, pp. 1-8, Feb. 1993.
17. Addis, T., D. Boulter, L.R. Ramisa and D. Plumb, "*The Quest for Borehole Stability in the Cusiana Field"*, pp. 33-43, Drilling April/July 1993.
18. AL-Rubaey,Abdulkareem Abbas."*Mechanical/Chemical Stresses affecting borehole Instability due to Interaction between Shale and Drilling Fluids*" PhD. Dissertation. Engineering collage, Baghdad University, Iraq. 2007.

Nomenclature :

λ:	hole azimuth, degree.
β:	hole angle, degree.
θ:	angle around wellbore, degree.
τ:	shear stress,psi.
σ:	normal stress, psi.
ν:	poisson's ratio.
$\sigma_{\theta\theta}$:	hoop (tangential) stress at wellbore, psi.
$\tau_{\theta z}$:	shear stress at wellbore, psi.
σ_h:	minimum horizontal stress, psi.
σ_H:	maximum horizontal stress, psi.
ΔP_π:	osmotic pressure potential, psi.
σ_r:	reflection coefficient.
$\tau_{r\theta}$:	shear stress at wellbore, psi.
σ_{rr}:	radial normal stress at wellbore, psi.
τ_{rz}:	shear stress at wellbore, psi.
σ_v:	overburden stress, psi.
σ_x:	normal stress in X-direction, psi.
τ_{xy}, τ_{yz}, τ_{zx}:	in-situ shear stress in (x, y, z) coordinated system, psi.
σ_y:	normal stress in Y-direction, psi.
σ_z:	axial stress, psi
σ_{zz}:	axial stress at wellbore, psi.
P_{nw}:	near wellbore pressure, psi.
P_o:	pore pressure, psi.
P_w:	well pressure, psi.
r:	near wellbore radius, ft.
r_w:	wellbore radius, ft.

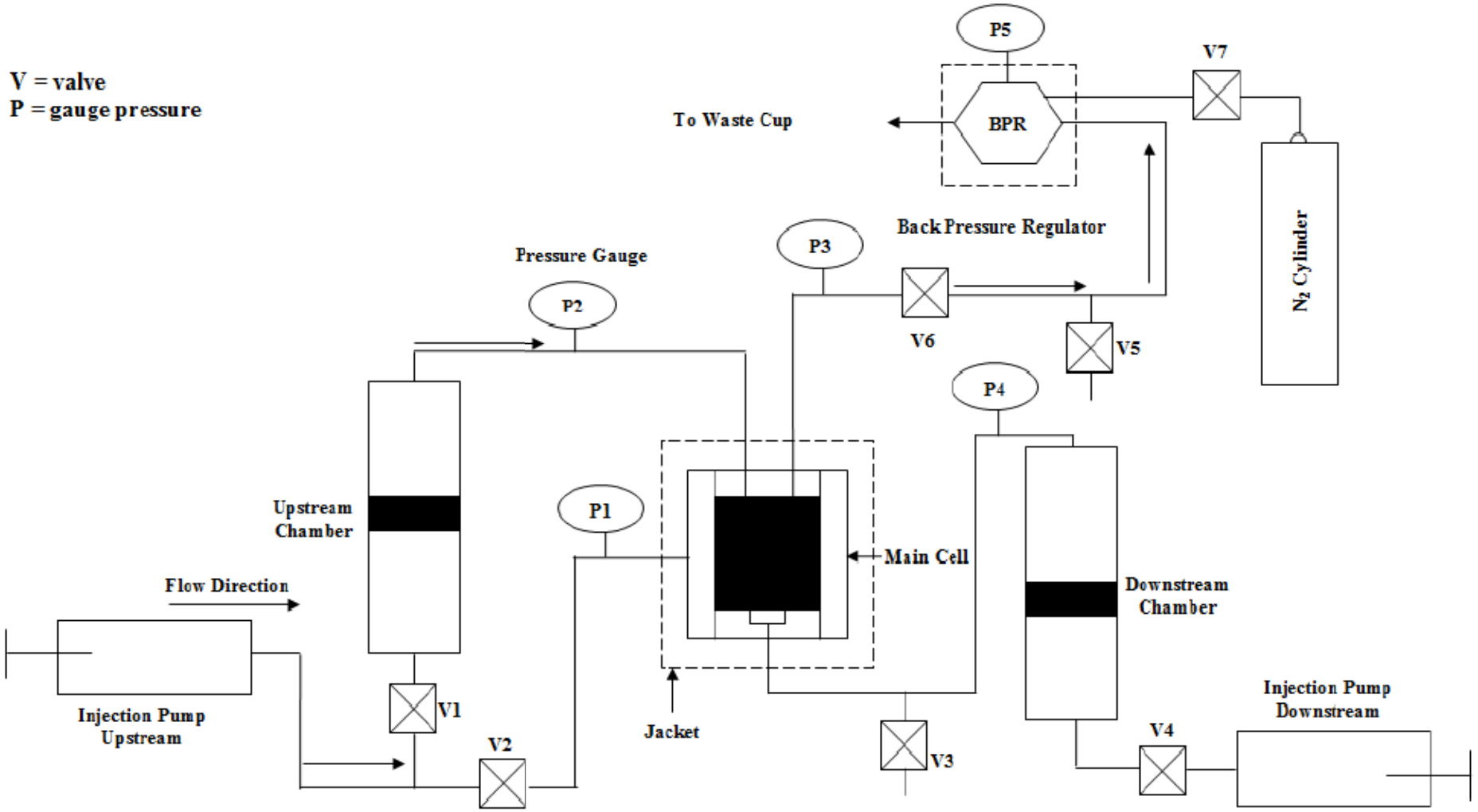

Figure (1): Experimental set up for Pressure Transmission Test (PPT)

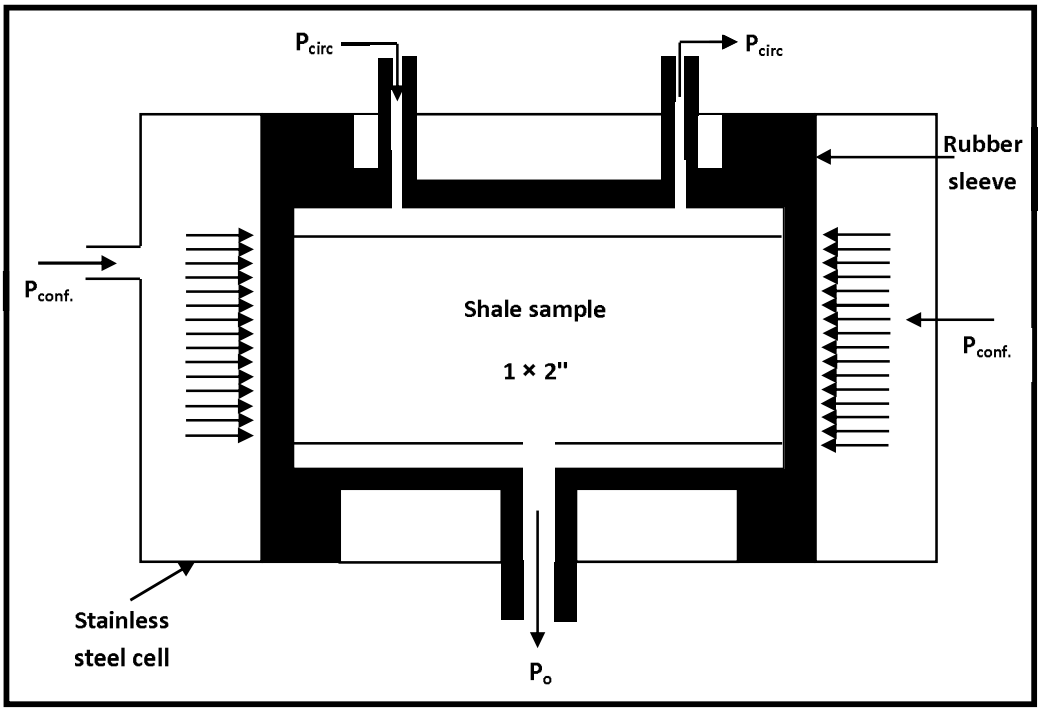

Figure (2): Schematic diagram of the pressure transmission test cell

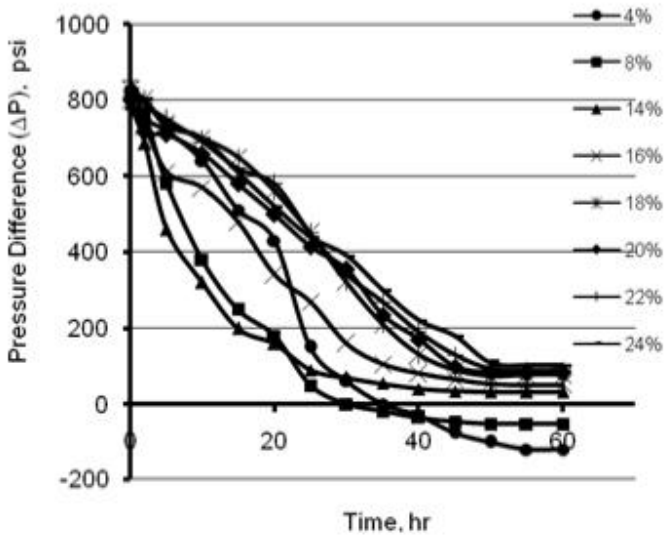

Figure (3): Osmotic Pressure Difference Versus %NaCl Salt Concentration Variations

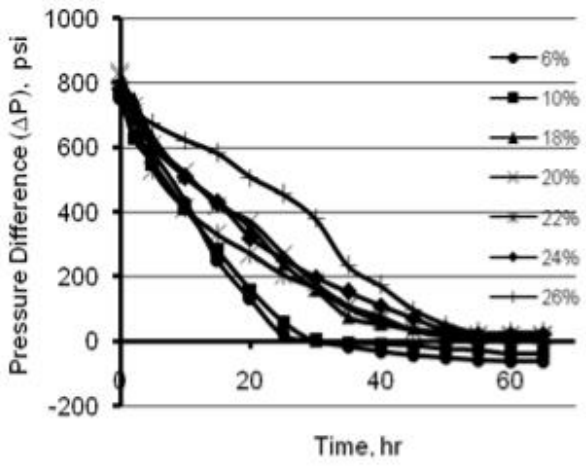

Figure (4): Osmotic Pressure Difference Versus %KCl Salt Concentration Variations

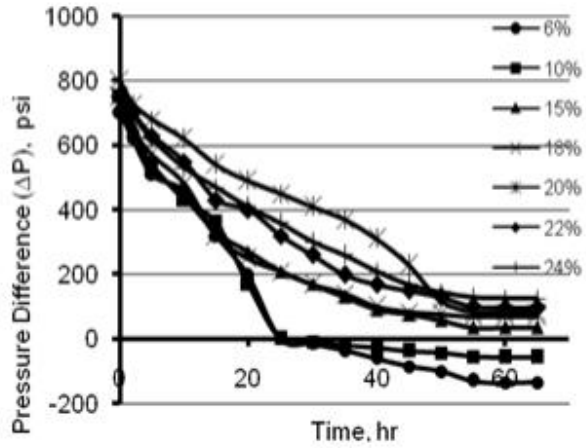

Figure (5): Osmotic Pressure Difference Versus %$CaCl_2$ Salt Concentration Variations

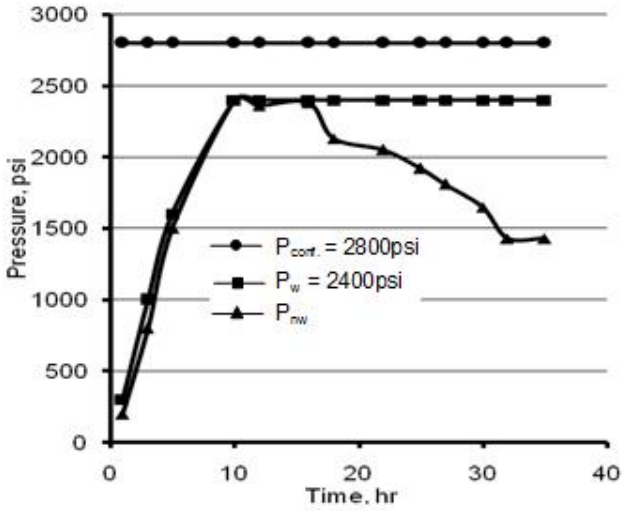

Figure (6): Near wellbore pressure variation with time for (14%) NaCl solution

Table (1): Membrane efficiency results

Salt type	Salt concent. %	Water activity %	ΔP, Theoretical pressure, psi	ΔP Observed pressure, psi	Membrane efficiency, I_m %
NaCl	4	0.98	- 1375.87	- 120	8.72
	8	0.95	- 698.83	- 52	7.44
	14	0.90	478.64	32	6.68
	16	0.88	968.05	52	5.37
	18	0.85	1723.41	78	4.52
	20	0.83	2241.94	82	3.66
	22	0.80	3043.65	90	2.96
	24	0.78	3595.01	103	2.86
KCl	6	0.98	- 1375.87	- 62	4.50
	10	0.96	- 926.84	- 38	4.09
	18	0.91	238.00	9	3.78
	20	0.89	721.97	16	2.21
	22	0.88	968.05	18	1.86
	24	0.86	1468.70	22	1.49
	26	0.84	1981.13	28	1.41
$CaCl_2$	6	0.98	- 1375.87	- 135	9.81
	10	0.95	- 698.83	- 57	8.15
	15	0.90	478.64	35	7.31
	18	0.86	1468.70	70	4.76
	20	0.83	2241.94	83	3.70
	22	0.80	3043.66	79	3.18
	24	0.76	4160.69	126	3.02

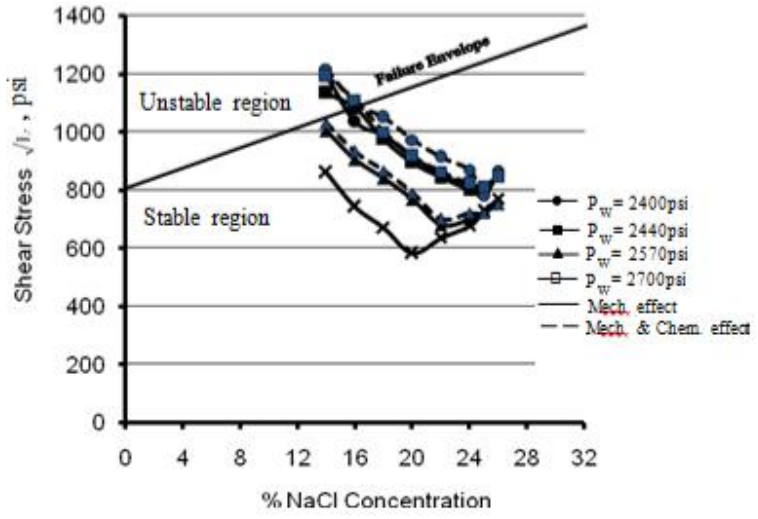

Figure (7): Invariant shear stress profile for % NaCl concentrations

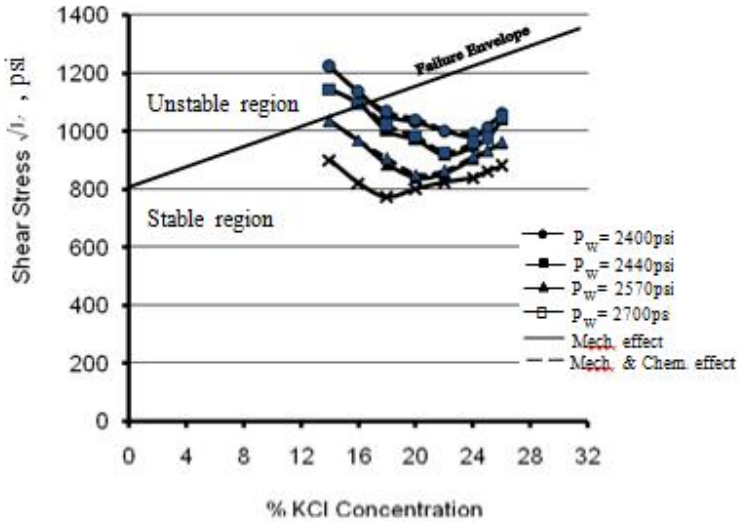

Figure (8): Invariant shear stress profile for % KCl concentrations

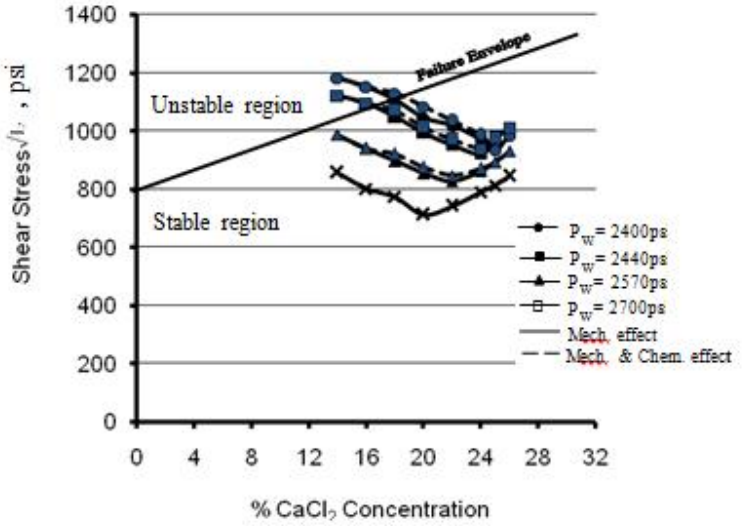

Figure (9): Invariant shear stress profile for % $CaCl_2$ concentration

Appendix

According to [Bradley, 1979] at the borehole wall when r = r_w, vertical hole, we get:

$$\sigma_x = (\sigma_h \cos^2 \lambda + \sigma_H \sin^2 \lambda) \cos^2 \beta + \sigma_v \sin^2 \beta$$

$$\sigma_x = (0.85 \cos^2 0 + 0.85 \sin^2 0) \cos^2 0 + 1 \sin^2 0$$

$$\sigma_x = (0.85 * 1 + 0.85 * 0) * 1 + 1 * 0 = 0.85 \text{ psi/ft}$$

$$\sigma_y = (\sigma_h \sin^2 \lambda + \sigma_H \cos^2 \lambda)$$

$$\sigma_y = (0.85 \sin^2 0 + 0.85 \cos^2 0)$$

$$\sigma_y = (0.85 * 0 + 0.85 * 1) = 0.85 \text{ psi/ft}$$

$$\sigma_z = (\sigma_h \cos^2 \lambda + \sigma_H \sin^2 \lambda) \sin^2 \beta + \sigma_v \cos^2 \beta$$

$$\sigma_z = (0.85 \cos^2 0 + 0.85 \sin^2 0) \sin^2 0 + 1 \cos^2 0$$

$$\sigma_z = (0.85 * 1 + 0.85 * 0) * 0 + 1 * 1 = 1 \text{ psi/ft}$$

$$\tau_{yz} = \sin \lambda \cos \lambda \sin \beta (\sigma_H - \sigma_h)$$

$$= \sin 0 \cos 0 \sin 0 (0.85 - 0.85) = 0$$

$$\tau_{xz} = \sin \beta \cos \beta (\sigma_h \cos^2 \lambda + \sigma_H \sin^2 \lambda - \sigma_v)$$

$$= \sin 0 \cos 0 (0.85 \cos^2 0 - 0.85 \sin^2 0 - 1) = 0$$

$$\tau_{oz} = 2 (\tau_{yz} \cos \theta - \tau_{xz} \sin \theta)$$

$$= 2 (0 * \cos 0 - 0 * \sin 0) = 0$$

$$\tau_{r\theta} = \tau_{rz} = 0$$

$$\sigma_x = \sigma_y = \sigma_H = \sigma_h = 0.85$$

$$\tau_{xy} = \tau_{yz} = \tau_{xz} = 0$$

For 14% NaCl, P_w = 2400 psi = 0.485 psi/ft = 1.12 gm/cc

$$P_{nw} = 1430 \text{ psi} = 0.2894 \text{ psi/ft.}$$

$$P_o = 0.45 \text{ psi/ft}, I_m = 0.0668.$$

$$\Delta P = P_{nw} - P_o = 0.2894 - 0.45 = 0.1606 \text{ psi/ft.}$$

The stresses around the wellbore wall are:

$$\sigma_{rr} = P_w - P_{nw} = 0.485 - 0.2894 = 0.1956 \text{ psi/ft.}$$

$$\sigma_{\theta\theta} = \sigma_x + \sigma_y - 2(\sigma_x - \sigma_y) \cos 2\theta - 4 \tau_{xy} \sin 2\theta + \alpha \Delta P - I_m \Delta P - P_w - P_{nw}$$

$$= 0.85 + 0.85 - 2 (0.85 - 0.85) \cos 0 - 4 * 0 \sin 0 + 0.9 (-0.1606)$$

$$+ 0.0668 (-0.1606) - 0.485 - 0.2894 = 0.79178 \text{ psi/ft.}$$

$$\sigma_{zz} = \sigma_z - \nu [(\sigma_x - \sigma_y) \cos 2\theta + 4 \tau_{xy} \sin 2\theta] + \alpha \Delta P - I_m \Delta P - P_w - P_{nw}$$

$$= 1 - 0.22 [2(0.85 - 0.85) \cos 0 + 4 * 0 \sin 0] + 0.9 (-0.1606)$$

– 0.0668 (–0.1606) – 0.2894 = 0.57678 psi/ft.

The effective stress (mean stress) is:

$$J_1 = \frac{\sigma_{rr}+\sigma_{\theta\theta}+\sigma_{zz}}{3} = \frac{0.1956+0.79178+0.57678}{3} = 0.52138 \quad psi/ft.$$

$J_1 = 0.52138 * 4940 = 2575$ psi

Also the invariant shear stress ($\sqrt{J_2}$) is:

$$\sqrt{J_2} = \frac{1}{3}\left(\sqrt{(\sigma_{rr}-\sigma_{\theta\theta})^2+(\sigma_{\theta\theta}-\sigma_{zz})^2+(\sigma_{zz}-\sigma_{rr})^2}\right)$$

$$\sqrt{J_2} = \frac{1}{3}\left(\sqrt{(0.1956-0.7917)^2+(0.7917-0.5767)^2+(0.5767-0.1956)^2}\right)$$

$$\sqrt{J_2} = 0.2464 \ psi/ft$$

$$\sqrt{J_2} = 0.2464 * 4940 = 1217 \ psi$$

If the chemical factors are neglected, i.e. ($I_m = 0$), then:

$\sigma_{rr} = P_w - P_{nw} = 0.485 - 0.2894 = 0.1956$ *psi/ft.*

$\sigma_{\theta\theta} = \sigma_x + \sigma_y - 2(\sigma_x - \sigma_y) \cos 2\theta - 4\ \tau_{xy} \sin 2\theta + \alpha\Delta P - P_w - P_{nw}$

$= 0.85 + 0.85 - 2\ (0.85 - 0.85) \cos 0 - 4 * 0 \sin 0 + 0.9\ (-0.1606) - 0.485 - 0.2894$

$= 0.7810$ *psi/ft.*

$\sigma_{zz} = \sigma_z - \nu\ [(\sigma_x - \sigma_y) \cos 2\theta + 4\ \tau_{xy} \sin 2\theta] + \alpha\Delta P - P_{nw}$

$= 1 - 0.22\ [2\ (0.85 - 0.85) \cos 0 + 4 * 0 \sin 0] + 0.9\ (-0.1606) - 0.2894 = 0.5660$ *psi/ft.*

$$J_1 = \frac{0.1956+0.7810+0.5660}{3} = 0.5142 \quad psi/ft.$$

$J_1 = 0.5142 * 4940 = 2540$ *psi*

$$\sqrt{J_2} = \frac{1}{3}\left(\sqrt{(0.1956-0.781)^2+(0.781+0.566)^2+(0.566+0.1956)^2}\right)$$

$\sqrt{J_2} = 0.2417$ *psi/ft,* So $\sqrt{J_2} = 0.2417 * 4940 = 1194$ *psi*